

# QUANTIZATION FOR DISTRIBUTED OPTIMIZATION

**Vineeth S**

VINEETHS@IISC.AC.IN

*Division of Electrical, Electronics, and Computer Sciences*

*Indian Institute of Science*

*Bangalore, India*

## Abstract

Massive amounts of data have led to the training of large-scale machine learning models on a single worker inefficient. Distributed machine learning methods such as Parallel-SGD have received significant interest as a solution to tackle this problem. However, the performance of distributed systems does not scale linearly with the number of workers due to the high network communication cost for synchronizing gradients and parameters. Researchers have proposed techniques such as quantization and sparsification to alleviate this problem by compressing the gradients. Most of the compression schemes result in compressed gradients that cannot be directly aggregated with efficient protocols such as all-reduce. In this paper, we present a set of all-reduce compatible gradient compression schemes which significantly reduce the communication overhead while maintaining the performance of vanilla SGD. We present the results of our experiments with the CIFAR10 dataset and observations derived during the process. Our compression methods perform better than the in-built methods currently offered by the deep learning frameworks. Code is available at the repository: <https://github.com/vineeths96/Gradient-Compression>.

**Keywords:** Distributed optimization, Large scale machine learning, Communication

# 1 Introduction

Deep learning models trained on large amounts of data have shown superhuman performance in tasks such as computer vision [1], speech [2], and natural language processing [3]. The remarkable success of these models is driven by the huge amounts of data available and the increase in model size [4][5]. As models and data grow in size, the process of training the models becomes very computation-intensive and thus time-consuming. In order to mitigate this problem, large-scale models are typically trained on a cluster of distributed workers to utilize the computing power of multiple workers [6][7]. This paradigm of parallel-SGD is commonly known as data parallelism. Distributed learning can be mathematically formulated as an optimization problem as follows:

$$\begin{aligned} \min_{\theta \in \mathbb{R}^d} f(\theta) &= \frac{1}{M} \sum_{m=1}^M f_m(\theta) \\ f_m(\theta) &= \mathbb{E}_{\mathbf{x}^n \sim \mathcal{D}^m} f(\theta; \mathbf{x}^n), \end{aligned} \tag{1}$$

where  $\theta \in \mathbb{R}^n$  denotes the model parameters to be learned,  $M$  is the number of workers,  $\mathcal{D}^m$  denotes the local data distribution at worker  $m$ , and  $f(\theta; \mathbf{x})$  is the loss function of the model on input  $\mathbf{x}$ . At each iteration, workers train a local copy of the model with a subset of the total data. We assume the standard optimization setting where every worker  $m$  can locally observe an unbiased stochastic gradient  $\mathbf{g}_t^m$ , such that  $\mathbb{E}[\mathbf{g}_t^m] = \nabla f_m(\theta_t)$  at iteration  $t$ . Workers sample the local stochastic gradients  $\mathbf{g}_t^m$  in parallel, and they synchronize them by averaging among the workers  $\mathbf{g}_t = \frac{1}{M} \sum_{m=1}^M \mathbf{g}_t^m$ . The model parameters are then iteratively updated using Stochastic Gradient Descent (SGD) or one of its variants with  $\theta_{t+1} = \theta_t - \eta_t \mathbf{g}_t$ , where  $\eta_t$  is the learning rate at iteration  $t$ .

With the increase in the number of workers, the time taken for computation significantly reduces. However, with the increase in the number of workers, the time incurred for synchronizing gradients and parameters increases. This communication time becomes a bottleneck in the training process and even can nullify the savings in computation time

[8][9][10]. This bottleneck becomes detrimental when distributed learning is performed on the edge, where devices are connected via a constraint network. Many methods have been proposed to mitigate these issues, which can be broadly classified into two categories - (i) *Quantization of gradients*, where workers locally quantize the gradient to a lower number of bits before communication [11][12][13] and (ii) *Sparsification of gradients*, where workers locally select a subset of gradient coordinates and communicate these values [14][9][15].

Though the schemes developed on top of these methods reduce the bits communicated at every communication significantly, most of the methods fail to support parallel aggregation. Quite often, the compressed gradient cannot be directly added without decompressing it first. For example, the output of quantization in [11] is a 3-tuple, and the output of sparsification in [14] is a 2-tuple. [16] identifies such gradient compression schemes whose outputs can not be hierarchically added to be non-linear. In such cases, each worker has to gather the compressed outputs of every other worker, decompress each gradient, and add them to obtain the aggregated gradient. This type of aggregation where each worker collects information from every other worker is called an all-gather operation. Modern collective communication libraries like NVIDIA NCCL provide efficient hierarchical parallel aggregation primitives such as all-reduce for dense vectors. Since non-linear gradient compression schemes do not support the all-reduce operation, we will have to use the all-gather operation. However, this limits the scalability of the algorithms as the communication times scales as  $\mathcal{O}(\log M)$  for all-reduce and  $\mathcal{O}(M)$  for all-gather with  $M$  workers. [17] showed that in order to utilize parallel aggregation for compressed domain gradients, the compression function should be commutable with the gradient aggregation. Compression functions that satisfy this property require a single decompression operation at the end of all-reduce, whereas those which does not will have  $M$  number of decompression operations at the end of all-gather. Clearly, we can see that distributed learning with all-gather does not scale well with a large number of workers compared with all-reduce.

**Contributions** We present a set of all-reduce compatible gradient compression algorithms — QSGDMaxNorm Quantization, QSGDMaxNormMultiScale Quantization, and its sparsified variants. We establish upper bounds on the variance introduced by the quantization schemes and prove its convergence for smooth convex functions. The proposed compres-

sion schemes can trade off between the communication costs and the rate of convergence. We empirically evaluate the performance of the compression methods by training deep neural networks on the CIFAR10 dataset [18]. We examine the performance of training ResNet50 (computation-intensive) model and VGG16 (communication-intensive) model with and without the compression methods. We also compare the scalability of these methods with the increase in the number of workers. We implement the compression framework in PyTorch [19].

## 2 Related Work

Recent research has proposed different solutions to tackle the problem of communication bottleneck. We focus on approaches related to gradient compression that aims to reduce the cost of communication. We look at the popular approaches of Quantization and Sparsification for gradient compression.

**Quantization** Typically, the gradients values are represented and communicated in 32-bit floating-point representation. Reducing the number of bits used to represent these values by quantizing them to lower-precision has been shown to reduce the cost of communication. [20] proposed 1-bit SGD and [13] proposed SignSGD, where the gradient values are reduced to their one-bit representation. Though they show promise in reducing the communication overhead, the quantization error may impair the rate of convergence. Multi-bit unbiased quantization studied in [11] and [21] allows the flexibility to trade-off between the communication cost and the convergence rate by choosing the number of bits for quantized representation. [22] presented an adaptive quantization scheme where the gradients were randomly rotated and then were uniformly quantized with dynamic ranges for each coordinate. [22] also proves that their quantization scheme almost attains the standard convergence rate of vanilla SGD. [23] derived lower bounds on the number of bits required to ensure the standard convergence rate of SGD and presented quantization schemes that almost attains these bounds. [21] and [24] incorporated the history of quantization error at the current quantization step. Other approaches in quantization schemes include gradient quantization to three levels [12], and the quantization of gradient differences [25].

**Sparsification** Sparsification approaches typically select and communicate a subset of the gradient coordinates. To avoid losing information, the gradients which are not communicated are accumulated over iterations and are communicated at some point. [26] proposed sparsification along with threshold quantization to send the gradients larger than a predefined constant threshold. However, choosing a proper threshold is hard in practice since different models could exhibit different behavior. [27] proposed to choose a fixed proportion of positive and negative gradient update and communicate them. [14] presented Gradient Dropping to sparsify the gradients by truncating the smallest gradient components based on their absolute value. Other approaches in sparsification schemes include communicating the Top K values of gradients [9], employing momentum correction for faster convergence [15], and random sparsification [28].

### 3 Preliminaries

We introduce some notations and definitions that are standard in convex optimization. We denote vectors with bold letters, such as  $\mathbf{x}$ .  $x_i$  represents the  $i^{\text{th}}$  coordinate of the  $\mathbf{x}$ . We denote the sign of  $t \in \mathbb{R}$  by  $\text{sign}(t)$  ( $-1$  if  $t < 0$ , or  $0$  if  $t = 0$ , and  $1$  if  $t > 0$ ). Throughout this paper,  $\log$  denotes base-2 logarithm.

**Definition 1 (Convexity)** We say that a function  $f : \mathbb{R}^n \rightarrow \mathbb{R}$  is convex if and only if

$$f(y) \geq f(x) + \langle \nabla f(x), y - x \rangle, \forall \mathbf{x}, \mathbf{y} \in \mathbb{R}^n. \quad (2)$$

**Definition 2 (L-smoothness)** We say that a function  $f : \mathbb{R}^n \rightarrow \mathbb{R}$  is  $L$ -smooth if its gradient is  $L$ -Lipschitz continuous,

$$\|\nabla f(\mathbf{x}) - \nabla f(\mathbf{y})\|_2 \leq L\|\mathbf{x} - \mathbf{y}\|_2, \forall \mathbf{x}, \mathbf{y} \in \mathbb{R}^n. \quad (3)$$

We consider the standard stochastic gradient descent setup for convex functions [29]. Let  $\Theta \subseteq \mathbb{R}^n$  be a closed and convex set. We wish to minimize  $f : \Theta \rightarrow \mathbb{R}$ , where  $f$  is an unknown, differentiable, convex, and  $L$ -smooth function. We assume access to stochastic

gradients  $\tilde{g}$  of  $f$ , such that  $\mathbb{E}[\tilde{g}(\boldsymbol{\theta})] = \nabla f(\boldsymbol{\theta})$ . We assume the stochastic gradients have a second moment upper bound  $B$ , such that  $\mathbb{E}[\|\tilde{g}(\boldsymbol{\theta})\|_2^2] \leq B$  for all  $\boldsymbol{\theta} \in \Theta$ . We assume the stochastic gradients have a variance upper bound  $\sigma^2$ , such that  $\mathbb{E}[\|\tilde{g}(\boldsymbol{\theta}) - \nabla f(\boldsymbol{\theta})\|_2^2] \leq \sigma^2$  for all  $\boldsymbol{\theta} \in \Theta$ .

Under this setup, we have the following result:

**Theorem 3** [29] *Let  $\Theta \subseteq \mathbb{R}^n$  be a closed and convex set. Let  $f : \Theta \rightarrow \mathbb{R}$  be an unknown, convex, and  $L$ -smooth function. Let  $\boldsymbol{\theta}_0 \in \Theta$  be an arbitrary initial point, and let  $R^2 = \sup_{\boldsymbol{\theta} \in \Theta} \|\boldsymbol{\theta} - \boldsymbol{\theta}_0\|^2$ . Given repeated and independent access to stochastic gradients with variance upper bound  $\sigma^2$ , projected SGD executed for  $T$  iterations with constant step-size  $\eta_t = \frac{1}{L+1/\gamma}$ , where  $\gamma = \frac{R}{\sigma} \sqrt{\frac{2}{T}}$  satisfies,*

$$\mathbb{E} \left[ f\left(\frac{1}{T} \sum_{t=0}^T \boldsymbol{\theta}_t\right) \right] - \min_{\boldsymbol{\theta} \in \Theta} f(\boldsymbol{\theta}) \leq R \sqrt{\frac{2\sigma^2}{T}} + \frac{LR^2}{T}. \quad (4)$$

For a distributed data parallel setup with  $M$  workers, we have the following result:

**Corollary 4** [11] *Let  $\Theta, f, L, \boldsymbol{\theta}_0, \gamma$ , and  $R$  be as defined in Theorem 3 and let  $\epsilon > 0$ . Suppose we execute projected SGD on  $M$  processors, each with access to independent stochastic gradients of  $f$  with second moment upper bound  $B$ , with step-size  $\eta_t = \frac{1}{L + \frac{\sqrt{M}}{\gamma}}$ . Then for  $T = O\left(R^2 \cdot \max\left(\frac{2B}{K\epsilon^2}, \frac{L}{\epsilon}\right)\right)$  iterations,*

$$\mathbb{E} \left[ f\left(\frac{1}{T} \sum_{t=0}^T \boldsymbol{\theta}_t\right) \right] - \min_{\boldsymbol{\theta} \in \Theta} f(\boldsymbol{\theta}) \leq \epsilon. \quad (5)$$

## 4 Algorithms

Consider a distributed learning setting with  $M$  workers. Each worker  $m$  have access to an unbiased stochastic gradient  $\mathbf{g}_t^m$ , such that  $\mathbb{E}[\mathbf{g}_t^m] = \nabla f_m(\boldsymbol{\theta}_t)$  at iteration  $t$ . Note that we consider the cost of compression and decompression of gradients, if any, to be included in the cost of communication.

In our experiments, we observed that coding schemes such as Elias Coding in [11] takes a significant amount of time to encode and decode millions of parameters, which is typical in deep neural networks. Coding schemes reduce the number of bits communicated, especially with sparse vectors. However, the time taken for coding and decoding dwarfs the gain in savings in bits communicated. We thus do not employ any such coding schemes.

#### 4.1 QSGDMaxNorm Quantization

We present a stochastic uniform quantization function similar to the quantization functions in [11][10]. The quantization function is given by  $Q_s(\mathbf{v}, \|\mathbf{w}\|_2)$ , where the scale  $s \geq 1$  is a tunable parameter, corresponding to the number of non-zero quantization levels. The value  $\log(s)$  represents the precision or the number of bits required to represent each coordinate when  $s$  quantization levels are used.

Consider any  $\mathbf{v} \in \{\mathbf{g}_t^m : m = 1 : M\}$  at a given iteration  $t$ , where each  $\mathbf{g}_t^m \in \mathbb{R}^n$ . We define  $\mathbf{w}$  as the stochastic gradient with the maximum  $L_2$  norm among the workers. Thus,  $\|\mathbf{w}\|_2 = \max_m \|\mathbf{g}_t^m\|_2$ . For  $\mathbf{v} \neq \mathbf{0}$ ,  $Q_s(\mathbf{v}, \|\mathbf{w}\|_2)$  is defined as,

$$Q_s(v_i, \|\mathbf{w}\|_2) = \|\mathbf{w}\|_2 \cdot \text{sign}(v_i) \cdot \xi_i(\mathbf{v}, \|\mathbf{w}\|_2, s), \quad (6)$$

where  $\xi_i(\mathbf{v}, \|\mathbf{w}\|_2, s)$  are independent random variables defined as below. Let  $0 \leq l < s$  be an integer such that,  $|v_i|/\|\mathbf{w}\|_2 \in [l/s, (l+1)/s)$ . Then,

$$\xi_i(\mathbf{v}, \|\mathbf{w}\|_2, s) = \begin{cases} l/s, & \text{with prob } 1 - p(\frac{|v_i|}{\|\mathbf{w}\|_2}, s) \\ (l+1)/s, & \text{otherwise} \end{cases}, \quad (7)$$

where  $p(a, s) = as - l$  for  $a \in [0, 1]$ . For  $\mathbf{v} = \mathbf{0}$ , we define  $Q_s(\mathbf{v}) = \mathbf{0}$ . After quantization, we only need  $r = \lceil \log(s) \rceil + 1$  bits to represent each coordinate. The scaling factor is typically represented in 32-bit floating point representation. Hence, the overall communication cost is  $32 + dr$  bits, which is much smaller than  $32d$  bits needed for original gradient.

---

**Algorithm 1** QSGDMaxNorm Quantization

---

- 1: **Input:** Local parameter vector  $\boldsymbol{\theta}_t$ , local data, learning rate  $\eta_t$ , and number of workers  $M$
  - 2: **procedure** QSGDMaxNorm( $\boldsymbol{\theta}_t$ )
  - 3:   **for all** worker  $m$  **do**
  - 4:      $\mathbf{g}_t^m \leftarrow \nabla f_m(\boldsymbol{\theta}_t)$  ▷ Stochastic gradient
  - 5:      $\|\mathbf{w}\|_2 \leftarrow \max_m \|\mathbf{g}_t^m\|_2$  ▷ Max AllReduce Norm
  - 6:      $\boldsymbol{\zeta}_t^m \leftarrow Q_s(\mathbf{g}_t^m, \|\mathbf{w}\|_2)$  ▷ Quantize gradient
  - 7:      $\hat{\boldsymbol{\zeta}}_t \leftarrow \frac{1}{M} \sum_{m=1}^M \boldsymbol{\zeta}_t^m$  ▷ AllReduce gradients
  - 8:      $\hat{\mathbf{g}}_t \leftarrow R_s(\hat{\boldsymbol{\zeta}}_t, \|\mathbf{w}\|_2)$  ▷ Reconstruct gradient
  - 9:      $\boldsymbol{\theta}_{t+1} \leftarrow \boldsymbol{\theta}_t - \eta_t \hat{\mathbf{g}}_t$  ▷ Update parameters
- 

At every iteration, each worker calculates  $Q_s(\mathbf{v}, \|\mathbf{w}\|_2)$  and expresses the output as a tuple  $(\|\mathbf{w}\|_2, \boldsymbol{\zeta})$ , where  $\boldsymbol{\zeta}$  is the vector containing  $sign(v_i) \cdot s \cdot \xi_i(\mathbf{v}, \|\mathbf{w}\|_2, s)$ . We can easily verify this gradient compression function is commutative with gradient aggregation, and hence this quantization scheme is all-reduce compatible. Once the compressed gradients are reduced, the workers reconstruct back the aggregated gradient and update their model parameters. The reconstructed vector is given by,

$$\hat{\mathbf{v}} = R_s(\boldsymbol{\zeta}, \|\mathbf{w}\|_2) = \|\mathbf{w}\|_2 \cdot \boldsymbol{\zeta} / s. \quad (8)$$

## 4.2 QSGDMaxNormMultiScale Quantization

We present a multi-scale stochastic uniform quantization function extending the quantization function presented in the previous section. We can represent values with higher precision using larger scales compared to using smaller scales, thus reducing the error introduced by quantization. We can intelligently choose a higher scale for a coordinate while ensuring that the bits required for its representation are equal to the bits required for the smallest scale representation. The quantization function is given by  $Q_{\underline{s}}(\mathbf{v}, \|\mathbf{w}\|_2)$ , where  $\underline{s} = \{s_i, i = 1 : N\}$  is the set of scales with each  $s_i \geq 1$  a tunable parameter corresponding to the number of non-zero quantization levels. The value  $\log(s_i)$  represents the precision or the number of bits required to represent each coordinate when  $s_i$  quantization levels are used.



Consider any  $\mathbf{v} \in \{\mathbf{g}_t^m : m = 1 : M\}$  at a given iteration  $t$ , where each  $\mathbf{g}_t^m \in \mathbb{R}^n$ . We define  $\mathbf{w}$  as the stochastic gradient with the maximum  $L_2$  norm among the workers. Thus,  $\|\mathbf{w}\|_2 = \max_m \|\mathbf{g}_t^m\|_2$ . For  $\mathbf{v} \neq \mathbf{0}$ ,  $Q_{\underline{s}}(\mathbf{v}, \|\mathbf{w}\|_2)$  is defined as,

$$Q_{\underline{s}}(v_i, \|\mathbf{w}\|_2) = \|\mathbf{w}\|_2 \cdot \text{sign}(v_i) \cdot \xi_i(\mathbf{v}, \|\mathbf{w}\|_2, s_i^*), \quad (9)$$

where  $s_i^*$  for each coordinate  $i$  is the largest scale  $s \in \underline{s}$  satisfying,

$$s \leq \frac{\|\mathbf{w}\|_2}{|v_i|} \min_j s_j, \quad (10)$$

and  $\xi_i(\mathbf{v}, \|\mathbf{w}\|_2, s)$  are independent random variables defined as below. Let  $0 \leq l < s$  be an integer such that,  $|v_i|/\|\mathbf{w}\|_2 \in [l/s, (l+1)/s)$ . Then,

$$\xi_i(\mathbf{v}, \|\mathbf{w}\|_2, s) = \begin{cases} l/s, & \text{with prob } 1 - p(\frac{|v_i|}{\|\mathbf{w}\|_2}, s), \\ (l+1)/s, & \text{otherwise} \end{cases}, \quad (11)$$

where  $p(a, s) = as - l$  for  $a \in [0, 1]$ . For  $\mathbf{v} = \mathbf{0}$ , we define  $Q_s(\mathbf{v}) = \mathbf{0}$ .

---

**Algorithm 2** QSGDMaxNormMultiScale Quantization
 

---

- 1: **Input:** Local parameter vector  $\boldsymbol{\theta}_t$ , local data, learning rate  $\eta_t$ , and number of workers  $M$
  - 2: **procedure** QSGDMaxNormMultiScale( $\boldsymbol{\theta}_t$ )
  - 3:   **for all** worker  $m$  **do**
  - 4:      $\mathbf{g}_t^m \leftarrow \nabla f_m(\boldsymbol{\theta}_t)$  ▷ Stochastic gradient
  - 5:      $\|\mathbf{w}\|_2 \leftarrow \max_m \|\mathbf{g}_t^m\|_2$  ▷ Max AllReduce Norm
  - 6:     Compute  $s^{*,m}$  ▷ Compute coordinate scales
  - 7:      $s^* \leftarrow \min_{m=1}^M s^{*,m}$  ▷ Scale sharing
  - 8:      $\zeta_t^m \leftarrow Q_{\underline{s}}(\mathbf{g}_t^m, \|\mathbf{w}\|_2)$  ▷ Quantize gradient with  $s^*$
  - 9:      $\zeta_t \leftarrow \frac{1}{M} \sum_{m=1}^M \zeta_t^m$  ▷ AllReduce gradients
  - 10:     $\hat{\mathbf{g}}_t \leftarrow R_{\underline{s}}(\zeta_t, \|\mathbf{w}\|_2)$  ▷ Reconstruct gradient with  $s^*$
  - 11:     $\boldsymbol{\theta}_{t+1} \leftarrow \boldsymbol{\theta}_t - \eta_t \hat{\mathbf{g}}_t$  ▷ Update parameters
- 

However, any arbitrary coordinate can be in different scales across different workers, making this scheme all-reduce incompatible. We propose a technique, which we call as *scale sharing*, which enables us to choose a common scale for a particular coordinate across the

workers. We define  $s_i^* = \min_m s_i^{*,m}$ , where  $s_i^{*,m}$  is the scale calculated for coordinate  $i$  in worker  $m$ . This sharing process is all-reduce compatible and has an additional overhead of communicating  $\lceil \log(N) \rceil$  bits per coordinate. After quantization, we only need  $r = \lceil \log(s) \rceil + 1 + \lceil \log(N) \rceil$  bits to represent each coordinate. The scaling factor is typically represented in 32-bit floating-point representation. Hence, the overall communication cost is  $32 + dr$  bits, which is much smaller than  $32d$  bits needed for the original gradient.

At every iteration, each worker calculates the scale vector  $s^{*,m}$  consisting of scales for every coordinate and performs scale sharing. The workers then calculate  $Q_s(\mathbf{v}, \|\mathbf{w}\|_2)$  and express the output as a tuple  $(\|\mathbf{w}\|_2, \zeta)$ , where  $\zeta$  is the vector containing  $\text{sign}(v_i) \cdot s_i^* \cdot \xi_i(\mathbf{v}, \|\mathbf{w}\|_2, s_i^*)$ . We can easily verify this gradient compression function is commutative with gradient aggregation, and hence this quantization scheme is all-reduce compatible. Once the compressed gradients are reduced, the workers reconstruct back the aggregated gradient and update their model parameters. The reconstructed vector is given by,

$$\hat{\mathbf{v}} = R_s(\zeta, \|\mathbf{w}\|_2) = \|\mathbf{w}\|_2 \cdot \zeta \cdot /s^*. \quad (12)$$

where  $\cdot /$  denotes element-wise division.

### 4.3 GlobalRandKMaxNorm Compression

We explore using sparsification approaches in conjunction with quantization schemes in our compression schemes. We sparsify the gradients by choosing  $K$  coordinates uniformly and apply the QSGDMaxNorm Quantization scheme on these coordinates to further reduce the communication costs.

### 4.4 GlobalRandKMaxNormMultiScale Compression

We explore using sparsification approaches in conjunction with quantization schemes in our compression schemes. We sparsify the gradients by choosing  $K$  coordinates uniformly and apply the QSGDMaxNormMultiScale Quantization scheme on these coordinates to further reduce the communication costs.

## 5 Convergence Guarantees

In this section, we provide convergence guarantees to the quantization schemes we introduced in the previous section for smooth and convex functions. We assume that all assumptions listed in Section 3 hold.

### 5.1 QSGDMaxNorm Quantization

Consider the QSGDMaxNorm Quantization presented in Section 4.1. We show the following results and provide convergence guarantees.

**Lemma 5 (Unbiasedness and Variance bound)** *For any  $\mathbf{v} \in \mathbb{R}^n$ , we have  $\mathbb{E}[Q_s(\mathbf{v}, \|\mathbf{w}\|_2)] = \mathbf{v}$  and  $\mathbb{E}[\|Q_s(\mathbf{v}, \|\mathbf{w}\|_2) - \mathbf{v}\|_2^2] \leq (1 + \min(\frac{n}{s^2}, \frac{\sqrt{n}}{s}))\|\mathbf{w}\|_2^2$ .*

**Proof** We first show unbiasedness of the quantization scheme. For any  $\mathbf{v} \in \mathbb{R}^n$  and any coordinate index  $i$  we have,

$$\begin{aligned} \mathbb{E}[Q_s(v_i, \|\mathbf{w}\|_2)] &= \mathbb{E}[\|\mathbf{w}\|_2 \cdot \text{sign}(v_i) \cdot \xi_i(\mathbf{v}, \|\mathbf{w}\|_2)] \\ &= \|\mathbf{w}\|_2 \cdot \text{sign}(v_i) \cdot \left( \frac{l}{s} * (1 - p\left(\frac{|v_i|}{\|\mathbf{w}\|_2}, s\right)) + \frac{l+1}{s} * p\left(\frac{|v_i|}{\|\mathbf{w}\|_2}, s\right) \right) \\ &= \|\mathbf{w}\|_2 \cdot \text{sign}(v_i) \cdot \frac{|v_i|}{\|\mathbf{w}\|_2} \\ &= v_i. \end{aligned}$$

We will now show the variance upper bound. Recall the definition of  $\xi_i(\mathbf{v}, \|\mathbf{w}\|_2, s)$ ,

$$\xi_i(\mathbf{v}, \|\mathbf{w}\|_2, s) = \begin{cases} l/s, & \text{with prob } 1 - p\left(\frac{|v_i|}{\|\mathbf{w}\|_2}, s\right) \\ (l+1)/s, & \text{otherwise} \end{cases}.$$

We can show,

$$\mathbb{E}[\xi_i(\mathbf{v}, \|\mathbf{w}\|_2, s)^2] = \mathbb{E}[\xi_i(\mathbf{v}, \|\mathbf{w}\|_2, s)]^2 + \text{Var}[(\xi_i(\mathbf{v}, \|\mathbf{w}\|_2, s))]$$

$$\begin{aligned}
&= \frac{v_i^2}{\|\mathbf{w}\|_2^2} + \frac{1}{s^2} p\left(\frac{|v_i|}{\|\mathbf{w}\|_2}, s\right) \left(1 - p\left(\frac{|v_i|}{\|\mathbf{w}\|_2}, s\right)\right) \\
&\leq \frac{v_i^2}{\|\mathbf{w}\|_2^2} + \frac{1}{s^2} p\left(\frac{|v_i|}{\|\mathbf{w}\|_2}, s\right).
\end{aligned}$$

We now upper bound the  $L_2$  norm of the quantized vector as,

$$\begin{aligned}
\mathbb{E}[\|Q_s(\mathbf{v}, \|\mathbf{w}\|_2)\|_2^2] &= \sum_{i=1}^n \mathbb{E}[\|\mathbf{w}\|_2^2 \xi_i(\mathbf{v}, \|\mathbf{w}\|_2, s)^2] \\
&\leq \|\mathbf{w}\|_2^2 \sum_{i=1}^n \left[ \frac{v_i^2}{\|\mathbf{w}\|_2^2} + \frac{1}{s^2} p\left(\frac{|v_i|}{\|\mathbf{w}\|_2}, s\right) \right] \\
&\leq \left(1 + \frac{1}{s^2} \sum_{i=1}^n p\left(\frac{|v_i|}{\|\mathbf{w}\|_2}, s\right)\right) \|\mathbf{w}\|_2^2 \\
&\leq \left(1 + \min\left(\frac{n}{s^2}, \frac{\|\mathbf{v}\|_1}{s\|\mathbf{w}\|_2}\right)\right) \|\mathbf{w}\|_2^2 \\
&\leq \left(1 + \min\left(\frac{n}{s^2}, \frac{\|\mathbf{v}\|_1}{s\|\mathbf{v}\|_2}\right)\right) \|\mathbf{w}\|_2^2 \\
&\leq \left(1 + \min\left(\frac{n}{s^2}, \frac{\sqrt{n}}{s}\right)\right) \|\mathbf{w}\|_2^2.
\end{aligned}$$

Using the above results we can derive the variance upper bound for the quantized vector,

$$\begin{aligned}
\mathbb{E}[\|Q_s(\mathbf{v}, \|\mathbf{w}\|_2) - \mathbf{v}\|_2^2] &\leq \mathbb{E}[\|Q_s(\mathbf{v}, \|\mathbf{w}\|_2)\|_2^2] - \|\mathbf{v}\|_2^2 \\
&\leq \min\left(\frac{n}{s^2}, \frac{\sqrt{n}}{s}\right) \|\mathbf{w}\|_2^2 + \|\mathbf{w}\|_2^2 - \|\mathbf{v}\|_2^2 \\
&\leq \left(1 + \min\left(\frac{n}{s^2}, \frac{\sqrt{n}}{s}\right)\right) \|\mathbf{w}\|_2^2.
\end{aligned}$$

This result means that if  $\tilde{g}(\boldsymbol{\theta})$  is a stochastic gradient with second moment upper bound  $B$ , then  $Q_s(\tilde{g}(\boldsymbol{\theta}), \|\mathbf{w}\|_2)$  is a stochastic gradient with upper bound  $\alpha B$ , where  $\alpha = 1 + \min\left(\frac{n}{s^2}, \frac{\sqrt{n}}{s}\right)$ . ■

Combining the results of Lemma 5 with Theorem 3 and Corollary 4, we have the following guarantee for QSGDMaxNorm Quantization:

**Theorem 6** Let  $\Theta, f, L, \boldsymbol{\theta}_0$ , and  $R$  be as in Theorem 3. Let  $\epsilon > 0$  and  $\gamma = \frac{R}{\tilde{B}} \sqrt{\frac{2}{T}}$  with  $\tilde{B} = \left(2 + \min\left(\frac{n}{s^2}, \frac{\sqrt{n}}{s}\right)\right) B$ . Suppose we run parallel QSGDMaxNorm with  $s$  quantization levels on  $M$  processors, each having access to independent stochastic gradients of  $f$  with a second moment upper bound  $B$ , with step-size  $\eta_t = \frac{1}{L + \frac{\sqrt{M}}{\gamma}}$ . Then for  $T = O\left(R^2 \cdot \max\left(\frac{2\tilde{B}}{K\epsilon^2}, \frac{L}{\epsilon}\right)\right)$  iterations,

$$\mathbb{E} \left[ f\left(\frac{1}{T} \sum_{t=0}^T \boldsymbol{\theta}_t\right) \right] - \min_{\boldsymbol{\theta} \in \Theta} f(\boldsymbol{\theta}) \leq \epsilon. \quad (13)$$

**Proof** Let  $\tilde{g}(\boldsymbol{\theta})$  and  $\tilde{h}(\boldsymbol{\theta})$  be the stochastic gradient and quantized stochastic gradient respectively ( $\tilde{h}(\boldsymbol{\theta}) = Q_s(\tilde{g}(\boldsymbol{\theta}), \|\mathbf{w}\|_2)$ ). Then we have,

$$\begin{aligned} \mathbb{E}[\|\tilde{h}(\boldsymbol{\theta}) - \nabla f(\boldsymbol{\theta})\|_2^2] &\leq \mathbb{E}[\|\tilde{h}(\boldsymbol{\theta}) - \tilde{g}(\boldsymbol{\theta})\|_2^2] + \mathbb{E}[\|\tilde{g}(\boldsymbol{\theta}) - \nabla f(\boldsymbol{\theta})\|_2^2] \\ &\leq \left(1 + \min\left(\frac{n}{s^2}, \frac{\sqrt{n}}{s}\right)\right) B + B \\ &= \left(2 + \min\left(\frac{n}{s^2}, \frac{\sqrt{n}}{s}\right)\right) B, \end{aligned}$$

where we use Lemma 5 and the second moment upper bound assumption of stochastic gradients. ■

## 5.2 QSGDMaxNormMultiScale Quantization

Consider the QSGDMaxNormMultiScale Quantization presented in Section 4.2. We show the following results and provide convergence guarantees.

**Lemma 7 (Unbiasedness and Variance bound)** For any  $\mathbf{v} \in \mathbb{R}^n$ , we have  $\mathbb{E}[Q_{\hat{s}}(\mathbf{v}, \|\mathbf{w}\|_2)] = \mathbf{v}$  and  $\mathbb{E}[\|Q_{\hat{s}}(\mathbf{v}, \|\mathbf{w}\|_2) - \mathbf{v}\|_2^2] \leq (1 + \min(\frac{n}{\hat{s}^2}, \frac{\sqrt{n}}{\hat{s}})) \|\mathbf{w}\|_2^2$ , where  $\hat{s} = \min_{s \in \underline{s}} s$ .

**Proof** The proof follows the same way as of proof for QSGDMaxNorm Quantization scheme and noting that  $\hat{s} = \min_{s \in \underline{s}} s$ . This result means that if  $\tilde{g}(\boldsymbol{\theta})$  is a stochastic gradient with second moment upper bound  $B$ , then  $Q_{\hat{s}}(\tilde{g}(\boldsymbol{\theta}), \|\mathbf{w}\|_2)$  is a stochastic gradient with upper bound  $\beta B$ , where  $\beta = 1 + \min\left(\frac{n}{\hat{s}^2}, \frac{\sqrt{n}}{\hat{s}}\right)$  and  $\hat{s} = \min_{s \in \underline{s}} s$ . ■

Combining the results of Lemma 7 with Theorem 3 and Corollary 4, we have the following guarantee for QSGDMaxNorm Quantization:

**Theorem 8** *Let  $\Theta, f, L, \theta_0$ , and  $R$  be as in Theorem 3. Let  $\epsilon > 0$  and  $\gamma = \frac{R}{B} \sqrt{\frac{2}{T}}$  with  $\tilde{B} = \left(2 + \min\left(\frac{n}{\hat{s}^2}, \frac{\sqrt{n}}{\hat{s}}\right)\right) B$ , where  $\hat{s} = \min_{s \in \underline{s}} s$ . Suppose we run parallel QSGDMaxNormMultiScale with  $\underline{s}$  set of quantization levels on  $M$  processors, each having access to independent stochastic gradients of  $f$  with a second moment upper bound  $B$ , with step-size  $\eta_t = \frac{1}{L + \frac{\sqrt{M}}{\gamma}}$ . Then for  $T = O\left(R^2 \cdot \max\left(\frac{2\tilde{B}}{K\epsilon^2}, \frac{L}{\epsilon}\right)\right)$  iterations,*

$$\mathbb{E} \left[ f\left(\frac{1}{T} \sum_{t=0}^T \theta_t\right) \right] - \min_{\theta \in \Theta} f(\theta) \leq \epsilon. \quad (14)$$

**Proof** The proof follows the same way as proof for the QSGDMaxNorm Quantization scheme. ■

## 6 Experiments

We implement our code in PyTorch [19] using NVIDIA NCCL communication library. Unfortunately, PyTorch or NCCL do not support tensors of arbitrary bit length. As of writing this paper, the framework supports tensors of data types: signed and unsigned 8-bit integer and 16-bit floating-point real number. We omit data types that have a bit width greater than equal to the default floating-point representation of gradients (32-bit). Obviously, it does not reduce the communication cost but adds additional computational overhead. [30] implemented a bit-packing scheme to efficiently pack the sign bits into a tensor to overcome this issue. In our experiments, we observed that even though bit-packing methods provide additional savings in bits communicated, the time taken to pack and unpack is significantly large. Hence, we chose not to perform any such methods and use the closest representation available.

We validate our approach with the image classification on the CIFAR10 dataset [18]. We examine the performance of training ResNet50 (computation-intensive) model and VGG16 (communication-intensive) model, with and without the compression methods. We train for 150 epochs with a batch size of 128 per worker (weak scaling). We use SGD optimizer with a momentum of 0.9 and weight decay of  $5 \times 10^{-4}$  in conjunction with Cosine Annealing LR [31] scheduler. We implement two-scale compression schemes for the multi-scale compressors explained in Section 4.2 and Section 4.4. Multi-scale compressors can be easily generalized from these two-scale compressors. We repeat the experiments five times and plot the mean and standard deviation for all graphs.

We begin with an explanation of the notations used for the plot legends in this section. *AllReduce-SGD* corresponds to the default gradient aggregation provided by PyTorch. *QSGD-MN* and *GRandK-MN* corresponds to *QSGDMaxNorm Quantization* (Section 4.1) and *GlobalRandKMaxNorm Compression* (Section 4.3) respectively. The precision or number of bits used for the representation follows it. *QSGD-MN-TS* and *GRandK-MN-TS* corresponds to *QSGDMaxNormMultiScale Quantization* (Section 4.2) and *GlobalRandKMaxNormMultiScale Compression* (Section 4.4) respectively, with two scales (*TS*) of compression. The precision or number of bits used for the representation of the two scales follows it. For the sparsified schemes, we choose the value of K as 10000 for all the experiments. We compare our methods with a recent all-reduce compatible gradient compression scheme *PowerSGD* [16] for Rank-1 compression and Rank-2 compression.

## 6.1 Benchmarking Methods

In this section, we compare the performance of our schemes with the native PyTorch aggregation and PowerSGD. Figures 1 and 2 show the training loss and test accuracy respectively, over the epochs during training.

From figures 1a and 2a, we can observe that our compression schemes perform as good as the AllReduce-SGD for ResNet50 architecture. We can observe that initially the sparsified methods perform better – even than AllReduce-SGD – but the non-sparsified methods perform better with time. From figure 1b and 2b, we can observe that even though

initially our compression schemes perform worse compared to Allreduce-SGD, with time, they perform as good as the Allreduce-SGD for VGG16 architecture. However, contrary to our observations for ResNet50 architecture, the sparsified methods do not perform better than Allreduce-SGD for the non-sparsified methods for VGG16 architecture.

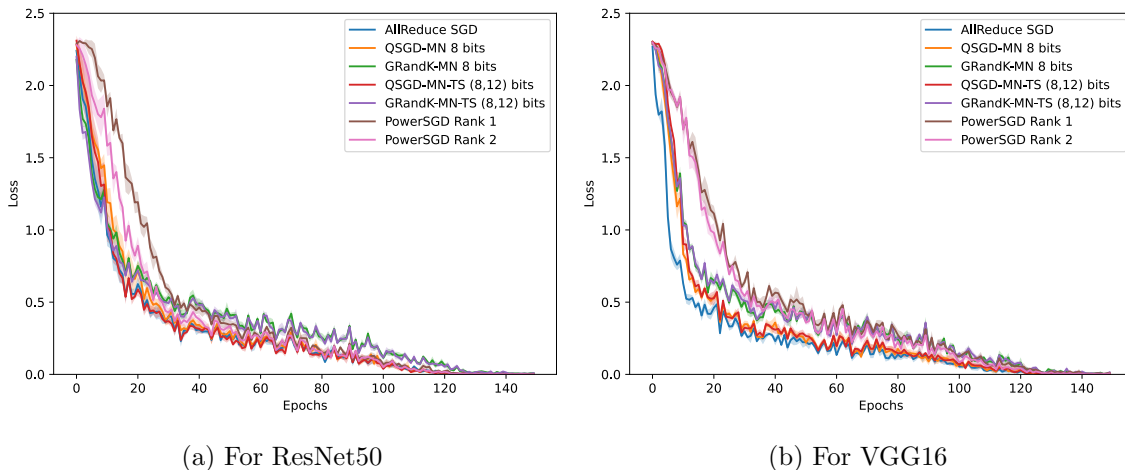


Figure 1: Benchmarking Methods: Loss vs Epoch

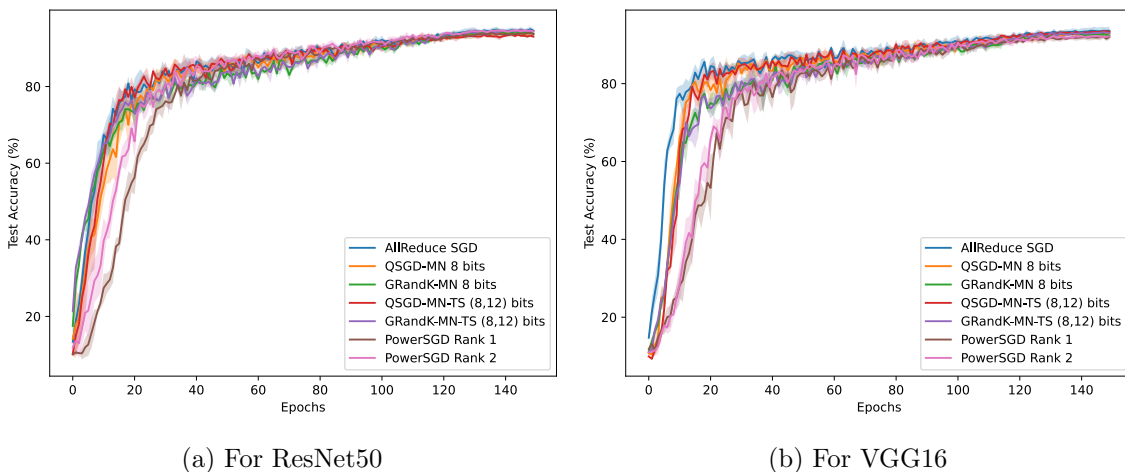


Figure 2: Benchmarking Methods: Accuracy vs Epoch

We can observe that all our methods significantly outperform PowerSGD for both ResNet50 and VGG16 architectures. This can be explained by the fact that PowerSGD uses a one-step power iteration method, which can introduce a large compression error. We can



also note that the two-scale QSGD-MN-TS performs better than the single-scale QSGD-MN – due to its reduced quantization error – once the training has passed its transient state.

## 6.2 QSGDMaxNorm Quantization

In this section, we compare the performance of the QSGDMaxNorm Quantization scheme with the native PyTorch aggregation for a varying number of quantization levels. More specifically, we evaluate the performance of this scheme as we vary the precision or the number of bits as  $\{8, 4, 2\}$ . Intuitively, one would expect the performance of the scheme to increase with precision. Figures 3 and 4 show the training loss and test accuracy respectively, over the epochs during training.

From figures 3a and 4a, we can observe that QSGD-MN schemes perform as good as the AllReduce-SGD for 8-bit and 4-bit quantization for the ResNet50 architecture. However, QSGD-MN with 2-bit quantization quantizes the gradients too aggressively. As a result, the training loss during the initial phase of training is significantly larger than the rest of the methods.

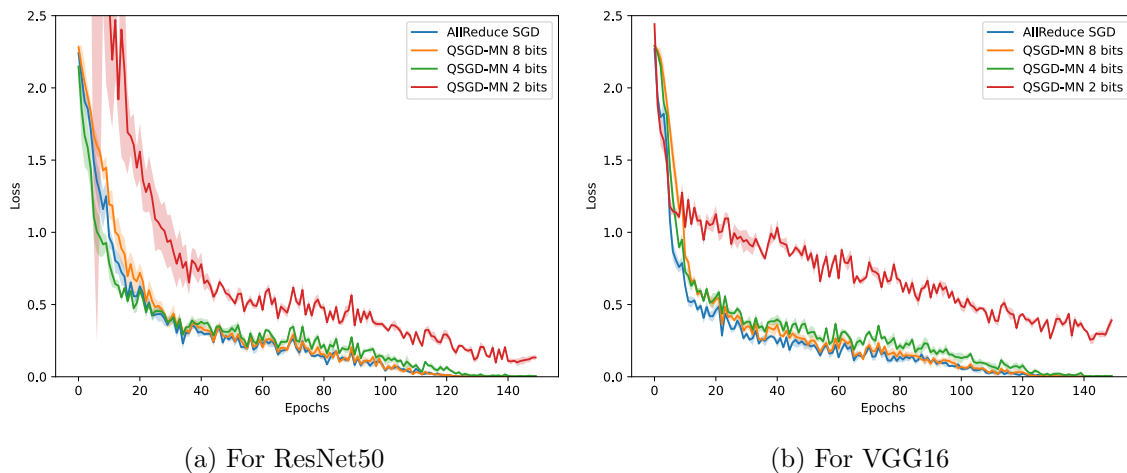


Figure 3: QSGDMaxNorm Quantization: Loss vs Epoch

From figures 3b and 4b, we can observe that QSGD-MN schemes perform as good as the AllReduce-SGD for 8-bit and 4-bit quantization for the VGG16 architecture. Even though QSGD-MN with 2-bit quantization quantizes the gradients too aggressively, the training

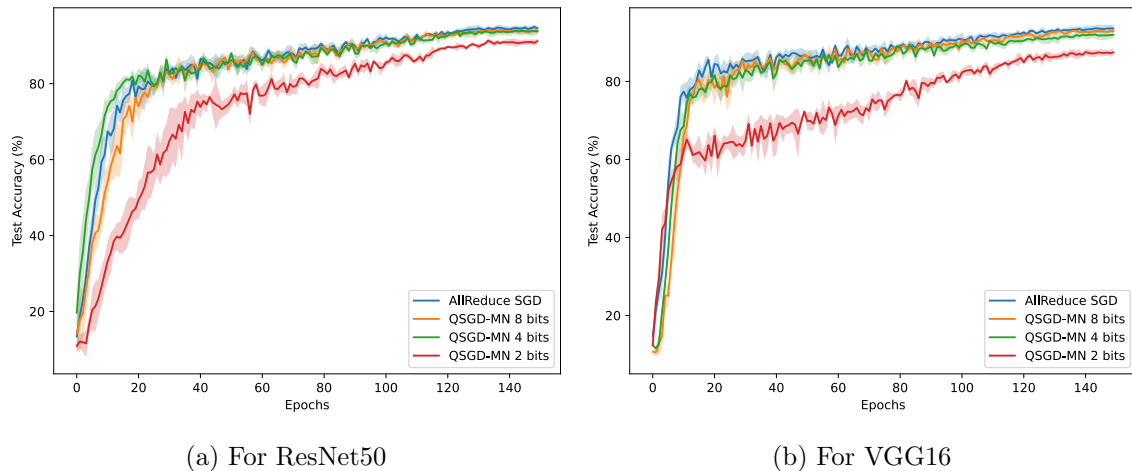


Figure 4: QSGDMaxNorm Quantization: Accuracy vs Epoch

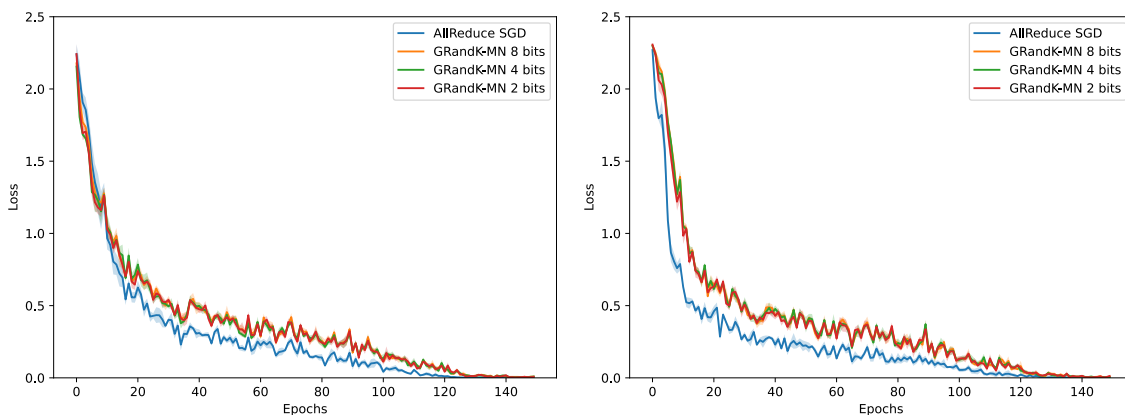
loss during the initial phase of training is comparable with the rest of the methods, unlike the case with ResNet50 architecture.

Though the loss decreases with increasing training epochs, there is a pronounced gap between the final loss of QSGD-MN with 2-bit quantization and the rest of the methods. This gap is more for VGG16 architecture compared to ResNet50 architecture. This effect is also reflected in the accuracy plots.

### 6.3 GlobalRandKMaxNorm Compression

In this section, we compare the performance of the GlobalRandKMaxNorm Compression scheme with the native PyTorch aggregation for a varying number of quantization levels. More specifically, we evaluate the performance of this scheme as we vary the precision or the number of bits as  $\{8, 4, 2\}$ . Figures 5 and 6 show the training loss and test accuracy respectively, over the epochs during training.

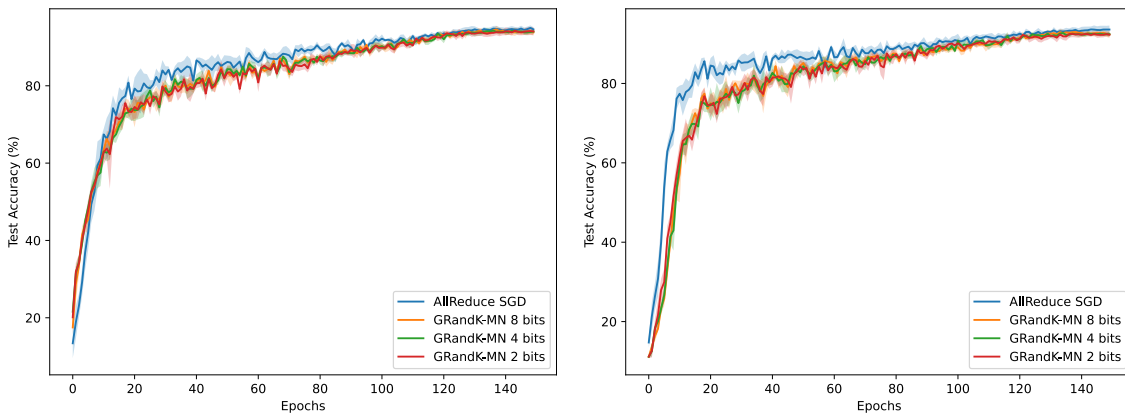
From figures 5a and 6a, we can observe that though initially, GRandK-MN schemes perform better than AllReduce-SGD, with time, the performance becomes worse for the ResNet50 architecture. From figures 5b and 6b, we can observe that GRandK-MN schemes perform worse compared to AllReduce-SGD throughout the training for the VGG16 architecture.



(a) For ResNet50

(b) For VGG16

Figure 5: GlobalRandKMaxNorm Compression: Loss vs Epoch



(a) For ResNet50

(b) For VGG16

Figure 6: GlobalRandKMaxNorm Compression: Accuracy vs Epoch

However, the performance improves towards the end of training. Interestingly, the performance seems to be resilient to the precision used. This behavior is expected because we communicate a very small random subset of the entire gradient.

### 6.4 QSGDMaxNormMultiScale Quantization

In this section, we compare the performance of the QSGDMaxNormMultiScale Quantization scheme with the native PyTorch aggregation for a varying number of two-scale quantization levels. More specifically, we evaluate the performance of this scheme as we vary the precision

or the number of bits as  $\{(8, 12), (6, 10), (4, 8), (2, 6)\}$ . Intuitively, one would expect the performance of the scheme to increase with precision. Figures 7 and 8 show the training loss and test accuracy respectively, over the epochs during training.

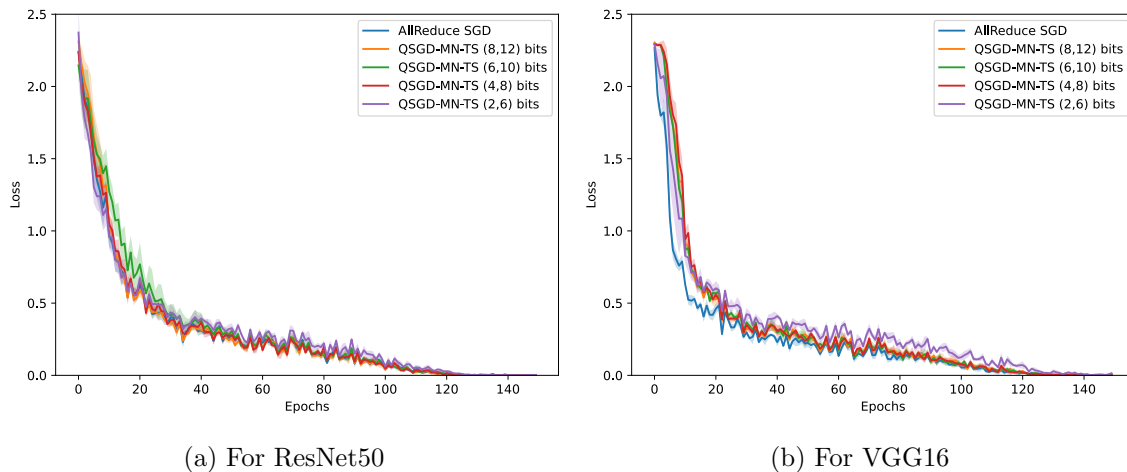


Figure 7: QSGDMaxNormMultiScale Quantization: Loss vs Epoch

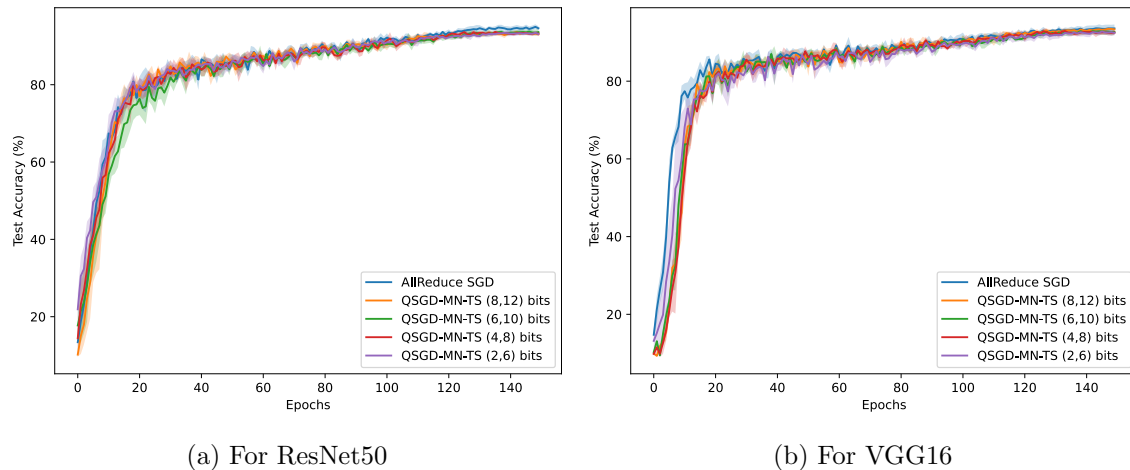


Figure 8: QSGDMaxNormMultiScale Quantization: Accuracy vs Epoch

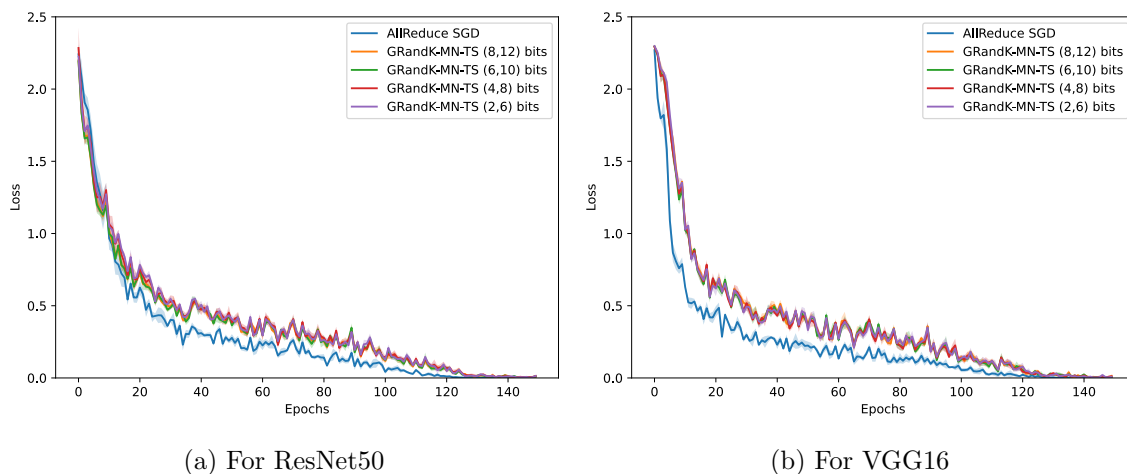
From figures 7a and 8a, we can observe that QSGD-MN-TS schemes perform as good as the AllReduce-SGD except for (6, 10) quantization for the ResNet50 architecture. Interestingly, the 2-bit quantization, which performed poorly in the single-scale scheme, performed in par with Allreduce-SGD in the two-scale scheme. From figures 7b and 8b, we can observe that QSGD-MN-TS schemes initially perform worse compared to AllReduce-SGD for

the VGG16 architecture. Similar to the case of ResNet50, the 2-bit quantization, which performed poorly in the single-scale scheme, performed in par with Allreduce-SGD in the two-scale scheme.

### 6.5 GlobalRandKMaxNormMultiScale Compression

In this section, we compare the performance of the GlobalRandKMaxNormMultiScale Compression scheme with the native PyTorch aggregation for a varying number of two-scale quantization levels. More specifically, we evaluate the performance of this scheme as we vary the precision or the number of bits as  $\{(8, 12), (6, 10), (4, 8), (2, 6)\}$ . Intuitively, one would expect the performance of the scheme to increase with precision. Figures 9 and 10 show the training loss and test accuracy respectively, over the epochs during training.

From figures 9a and 10a, we can observe that though initially, GRandK-MN-TS schemes perform better than AllReduce-SGD, with time, the performance becomes worse for the ResNet50 architecture. From figures 9b and 10b, we can observe that GRandK-MN-TS schemes perform worse compared to AllReduce-SGD throughout the training for the VGG16 architecture.



(a) For ResNet50 (b) For VGG16  
 Figure 9: GlobalRandKMaxNormMultiScale Compression: Loss vs Epoch

However, the performance improves towards the end of training. Interestingly, the performance seems to be resilient to the precision used. This behavior is expected because

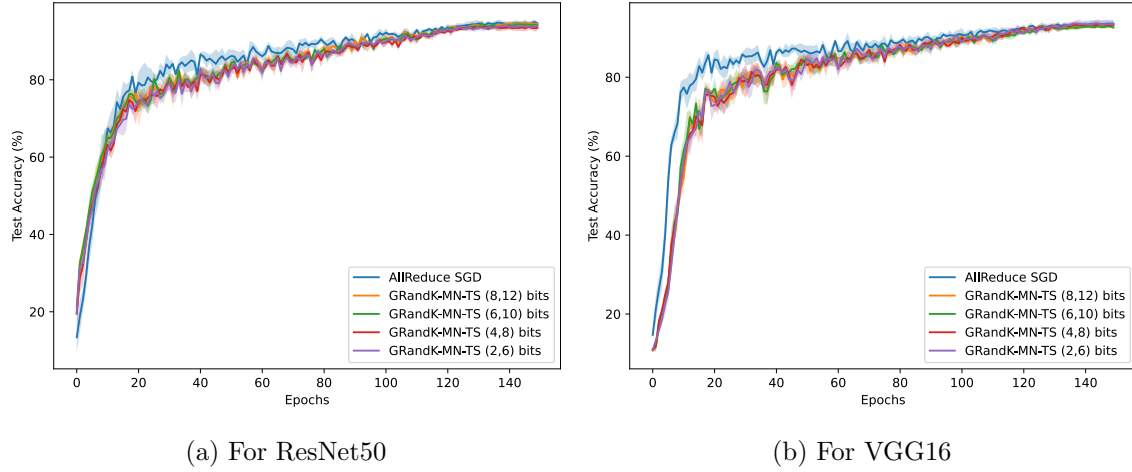


Figure 10: GlobalRandKMaxNormMultiScale Compression: Accuracy vs Epoch

we communicate a very small random subset of the entire gradient. These are similar to the observations made for GlobalRandKMaxNorm Compression.

## 6.6 Performance Modeling

We use the performance model developed in [12] to analyze the scalability of the compression schemes. We perform lightweight profiling on an AWS p3.8xlarge instance with 4 NVIDIA V100 GPUs. This instance supports NVLink GPU Peer to Peer Communication and has a network bandwidth of 10 Gbps. We then use this analytical model to study the throughput (images processed per second) for a cluster of 32 nodes, each equipped with 4 NVIDIA V100 GPUs with NVLink GPU interconnect.

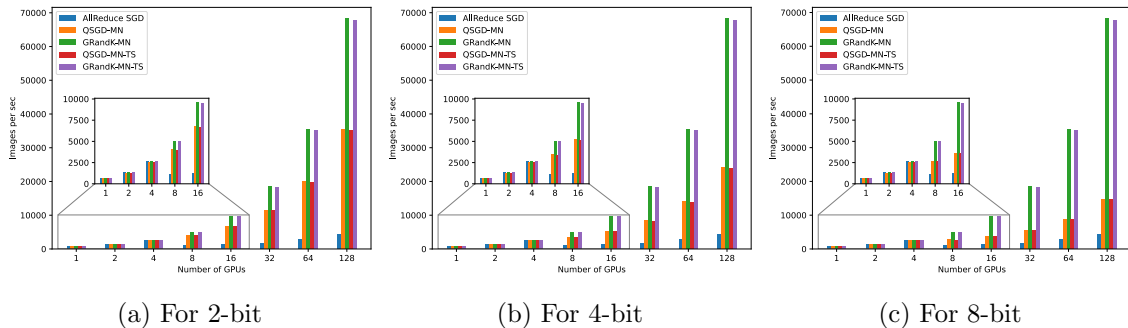


Figure 11: Performance Modeling: ResNet50 with 1 Gbps Ethernet

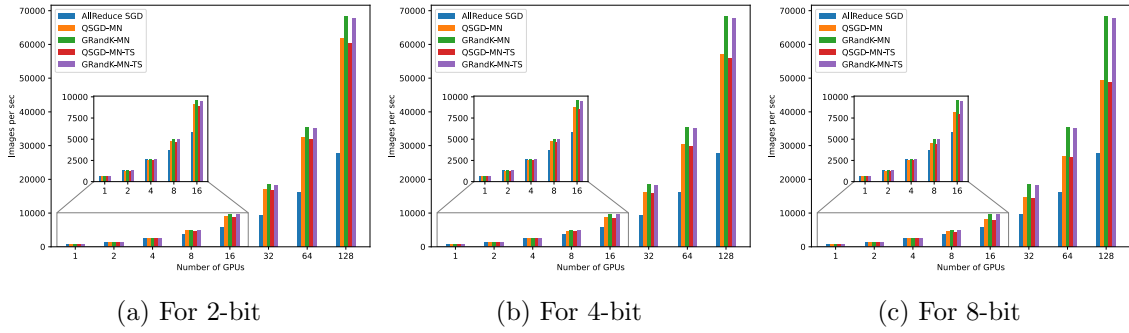


Figure 12: Performance Modeling: ResNet50 with 10 Gbps Ethernet

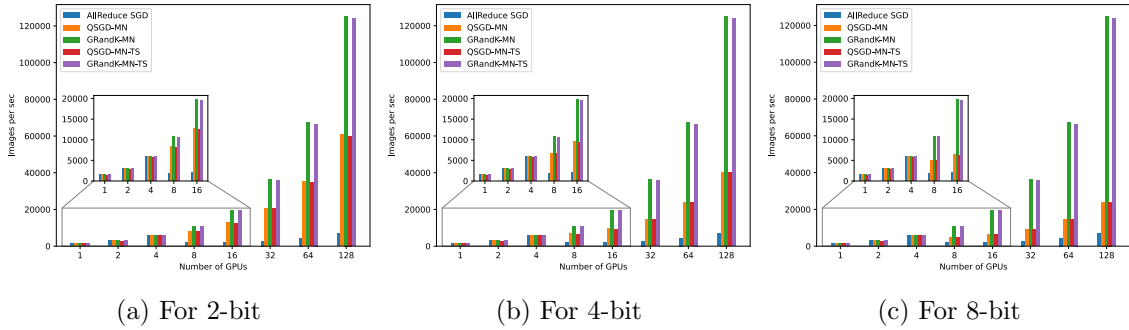


Figure 13: Performance Modeling: VGG16 with 1 Gbps Ethernet

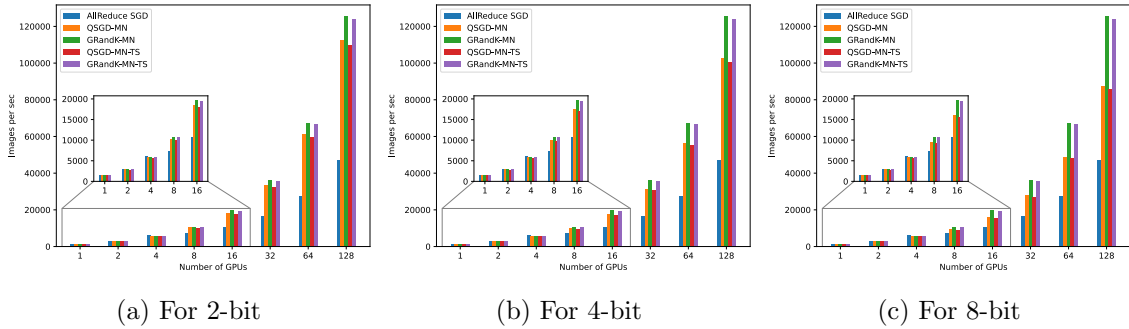


Figure 14: Performance Modeling: VGG16 with 10 Gbps Ethernet

We evaluate the performance under 1 Gbps and 10 Gbps Ethernet connection between the nodes. Under each condition, we vary the number of bits of quantization in  $\{2, 4, 8\}$ . For the two-scale compressors, this corresponds to the minimum value of the scales. Note that the framework currently does not support 2-bit or 4-bit tensors as of writing this paper and these results are not realizable currently.

Figures 11 and 12 shows the system throughput under 1 Gbps and 10 Gbps Ethernet connections for the ResNet50 architecture. Figures 13 and 14 shows the system throughput under 1 Gbps and 10 Gbps Ethernet connections for VGG16 architecture. We observe that our compression schemes have non-trivial speedup compared to the native synchronous SGD. The throughput decreases with an increase in the number of bits used for quantization. Under low bandwidth 1 Gbps Ethernet connection, sparsified methods significantly outperform the non-sparsified methods because of reduced communication. The speedup gain in VGG16 architecture is more than of ResNet50 architecture because the former is a communication-intensive model and the latter is a computation-intensive model. Compression schemes help to increase the system throughput when communication-to-computation ratio of the model is higher and the network bandwidth is lower.

## 6.7 Time Breakdown

In this section, we provide justifications for the non-trivial speedup in the distributed learning when compressors are employed. Figures 15a and 15b shows the time breakdown for various sub-processes in the training for ResNet50 architecture and VGG16 architecture respectively. We measure the times from a cluster of 4 machines, each with an NVIDIA V100 GPU.

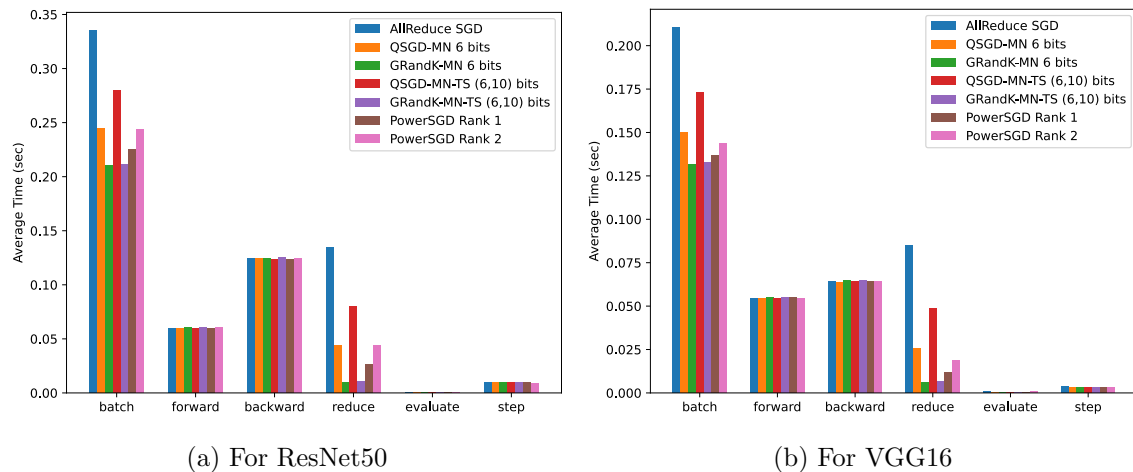


Figure 15: Time Breakdown of Compression methods



We can observe that the differences in training times arise due to the differences in the communication time. Observe that the two-scale methods have larger communication times because of two all-reduce operations of 8-bit tensors. The framework currently does not support tensors less than 8-bit as of writing this paper, and this increases the communication time for the two-scale methods. We expect that this time should decrease when the framework supports tensors of lower bit-width. We can also observe from the figures that the QSGDMaxNorm Quantization takes the same amount of time of PowerSGD compression with Rank-2 approximation, while ensuring better convergence and performance for ResNet50 architecture. QSGDMaxNorm Quantization takes slightly more time than PowerSGD compression with Rank-2 approximation for VGG16 architecture. This behavior can be explained by the fact that ResNet50 architecture has 23520842 parameters and VGG16 architecture has 14728266 parameters. A larger number of parameters would require more time to calculate low-rank approximations.

## 7 Concluding Remarks

With the increasing compute power of hardware systems, communication will soon be the bottleneck of large-scale learning. In this paper, we presented a set of all-reduce compatible gradient compression schemes which reduce the communication costs in distributed data-parallel machine learning. We establish upper bounds on the variance introduced by the proposed quantization schemes. We further establish the convergence of the quantization schemes for smooth and convex objective functions. The schemes allow to trade-off between the convergence and the communication costs by varying the number of quantization levels. We also conduct extensive experiments on practical deep learning models and evaluate the performance of the quantization schemes.

We present some generic observations and discussions on the usage of gradient compression for distributed machine learning.

**Necessity of gradient compression** While gradient compression methods significantly reduce communication costs in terms of bits, the gain in terms of time may not be significant. Many gradient compression schemes such as Top-K take a significant amount of

time to compress the gradients. The savings in bits may be attractive in federated learning, but they are not in data center training. Modern multi-node data center environments have upwards of 300 GBps GPU interconnect (such as NVIDIA NVLink3) and upwards of 10 Gbps Ethernet connection. Under these conditions, if the time taken for compressing and communicating the gradients is more than communicating the gradients without the compression, there is no necessity of using compression schemes.

**All-reduce vs All-gather** All-reduce communication primitive provides an efficient aggregation method to communicate between the workers compared to all-gather communication primitive. As a result, gradient compression schemes that are all-reduce compatible provide much better scaling. However, most of the current gradient schemes are not all-reduce compatible, which results in poor scaling with the number of workers.

**Computation-intensive training** Computation-intensive training limits the acceleration and performance gains with gradient compression. A training can be computation-intensive if we train a complex model or have a large batch size. In either case, the amount of time spent in computing can be much larger than the time spent in communication. This results in diminished performance gains when using gradient compression. On the other hand, communication-intensive training can gain significantly using gradient compression schemes. Given the rate at which hardware compute power is growing, most training in the future will be bottlenecked by communication, and gradient compression methods can play a crucial role in alleviating it.

**Limitations of the framework** Currently, the deep learning frameworks and communication libraries support only a limited range of tensor datatypes. Any compression schemes which use a representation that is not supported will have to use the next largest representation supported. This typically results in wastage of bits and hampers the performance gain. For example, the smallest representation supported by these frameworks are 8-bit tensors. If we wish to use 2-bit or 4-bit tensors, we will have to use 8-bit tensors. One way to mitigate this issue is to pack multiple coordinates to a dense tensor – which usually takes time and makes the scheme all-reduce incompatible. However, this issue will be resolved if the framework supports tensors of arbitrary bit-width.

## Acknowledgments

The author would like to thank Himanshu Tyagi for suggesting the problem, useful discussions, and guidance throughout this work. This work has been supported by a research grant from the Robert Bosch Center for Cyber-Physical Systems (RBCCPS) at the Indian Institute of Science, Bangalore.

## References

- [1] Kaiming He, Xiangyu Zhang, Shaoqing Ren, and Jian Sun. Deep residual learning for image recognition, 2015.
- [2] Xiaodong Cui, Vaibhava Goel, and George Saon. Embedding-based speaker adaptive training of deep neural networks, 2017.
- [3] Ashish Vaswani, Noam Shazeer, Niki Parmar, Jakob Uszkoreit, Llion Jones, Aidan N. Gomez, Lukasz Kaiser, and Illia Polosukhin. Attention is all you need, 2017.
- [4] Trishul Chilimbi, Yutaka Suzue, Johnson Apacible, and Karthik Kalyanaraman. Project adam: Building an efficient and scalable deep learning training system. In *11th USENIX Symposium on Operating Systems Design and Implementation (OSDI 14)*, pages 571–582, Broomfield, CO, October 2014. USENIX Association. ISBN 978-1-931971-16-4. URL <https://www.usenix.org/conference/osdi14/technical-sessions/presentation/chilimbi>.
- [5] Eric P. Xing, Qirong Ho, Wei Dai, Jin Kyu Kim, Jinliang Wei, Seunghak Lee, Xun Zheng, Pengtao Xie, Abhimanu Kumar, and Yaoliang Yu. Petuum: A new platform for distributed machine learning on big data, 2015.
- [6] Martin Abadi, Paul Barham, Jianmin Chen, Zhifeng Chen, Andy Davis, Jeffrey Dean, Matthieu Devin, Sanjay Ghemawat, Geoffrey Irving, Michael Isard, Manjunath Kudlur, Josh Levenberg, Rajat Monga, Sherry Moore, Derek G. Murray, Benoit Steiner, Paul Tucker, Vijay Vasudevan, Pete Warden, Martin Wicke, Yuan Yu, and Xiaoqiang Zheng.

- Tensorflow: A system for large-scale machine learning. OSDI'16, USA, 2016. USENIX Association. ISBN 9781931971331.
- [7] Ron Bekkerman, Mikhail Bilenko, and John Langford. *Scaling up Machine Learning: Parallel and Distributed Approaches*. Cambridge University Press, USA, 2011. ISBN 0521192242.
- [8] Feng Niu, Benjamin Recht, Christopher Re, and Stephen J. Wright. Hogwild!: A lock-free approach to parallelizing stochastic gradient descent, 2011.
- [9] Dan Alistarh, Torsten Hoefler, Mikael Johansson, Sarit Khirirat, Nikola Konstantinov, and Cédric Renggli. The convergence of sparsified gradient methods, 2018.
- [10] Ananda Theertha Suresh, Felix X. Yu, Sanjiv Kumar, and H. Brendan McMahan. Distributed mean estimation with limited communication, 2017.
- [11] Dan Alistarh, Demjan Grubic, Jerry Li, Ryota Tomioka, and Milan Vojnovic. Qsgd: Communication-efficient sgd via gradient quantization and encoding, 2017.
- [12] Wei Wen, Cong Xu, Feng Yan, Chunpeng Wu, Yandan Wang, Yiran Chen, and Hai Li. Terngrad: Ternary gradients to reduce communication in distributed deep learning, 2017.
- [13] Jeremy Bernstein, Yu-Xiang Wang, Kamyar Azizzadenesheli, and Anima Anandkumar. signsgd: Compressed optimisation for non-convex problems, 2018.
- [14] Alham Fikri Aji and Kenneth Heafield. Sparse communication for distributed gradient descent. *Proceedings of the 2017 Conference on Empirical Methods in Natural Language Processing*, 2017. doi: 10.18653/v1/d17-1045. URL <http://dx.doi.org/10.18653/v1/D17-1045>.
- [15] Yujun Lin, Song Han, Huizi Mao, Yu Wang, and William J. Dally. Deep gradient compression: Reducing the communication bandwidth for distributed training, 2020.
- [16] Thijs Vogels, Sai Praneeth Karimireddy, and Martin Jaggi. Powersgd: Practical low-rank gradient compression for distributed optimization, 2020.

- [17] Mingchao Yu, Zhifeng Lin, Krishna Narra, Songze Li, Youjie Li, Nam Sung Kim, Alexander Schwing, Murali Annavaram, and Salman Avestimehr. Gradiveq: Vector quantization for bandwidth-efficient gradient aggregation in distributed cnn training, 2018.
- [18] Alex Krizhevsky. Learning multiple layers of features from tiny images. *University of Toronto*, 05 2012.
- [19] Adam Paszke, Sam Gross, Francisco Massa, Adam Lerer, James Bradbury, Gregory Chanan, Trevor Killeen, Zeming Lin, Natalia Gimelshein, Luca Antiga, Alban Desmaison, Andreas Köpf, Edward Yang, Zach DeVito, Martin Raison, Alykhan Tejani, Sasank Chilamkurthy, Benoit Steiner, Lu Fang, Junjie Bai, and Soumith Chintala. Pytorch: An imperative style, high-performance deep learning library, 2019.
- [20] Frank Seide, Hao Fu, Jasha Droppo, Gang Li, and Dong Yu. 1-bit stochastic gradient descent and application to data-parallel distributed training of speech dnns. In *Interspeech 2014*, September 2014.
- [21] Jiaxiang Wu, Weidong Huang, Junzhou Huang, and Tong Zhang. Error compensated quantized sgd and its applications to large-scale distributed optimization, 2018.
- [22] Prathamesh Mayekar and Himanshu Tyagi. Ratq: A universal fixed-length quantizer for stochastic optimization, 2019.
- [23] Prathamesh Mayekar and Himanshu Tyagi. Limits on gradient compression for stochastic optimization, 2020.
- [24] Hanlin Tang, Xiangru Lian, Chen Yu, Tong Zhang, and Ji Liu. Doublesqueeze: Parallel stochastic gradient descent with double-pass error-compensated compression, 2020.
- [25] Konstantin Mishchenko, Eduard Gorbunov, Martin Takáč, and Peter Richtárik. Distributed learning with compressed gradient differences, 2019.
- [26] N. Strom. Scalable distributed dnn training using commodity gpu cloud computing. In *INTERSPEECH*, 2015.

- [27] Nikoli Dryden, Sam Ade Jacobs, Tim Moon, and Brian Van Essen. Communication quantization for data-parallel training of deep neural networks. In *Proceedings of the Workshop on Machine Learning in High Performance Computing Environments*, MLHPC '16, page 1–8. IEEE Press, 2016. ISBN 9781509038824.
- [28] Jianqiao Wangni, Jialei Wang, Ji Liu, and Tong Zhang. Gradient sparsification for communication-efficient distributed optimization, 2017.
- [29] Sébastien Bubeck. Convex optimization: Algorithms and complexity, 2015.
- [30] Jeremy Bernstein, Jiawei Zhao, Kamyar Azizzadenesheli, and Anima Anandkumar. signsgd with majority vote is communication efficient and fault tolerant, 2019.
- [31] Ilya Loshchilov and Frank Hutter. Sgdr: Stochastic gradient descent with warm restarts, 2017.